Chapter 6
Optical Detection of Non-amplified Genomic DNA

Di Li and Chunhai Fan

Abstract Nucleic acid sequences are unique to every living organisms including animals, plants and even bacteria and virus, which provide a practical molecular target for the identification and diagnosis of various diseases. DNA contains heterocyclic rings that has inherent optical absorbance at 260 nm, which is widely used to quantify single and double stranded DNA in biology. However, this simple quantification method could not differentiate sequences; therefore it is not suitable for sequence-specific analyte detection. In addition to a few exceptions such as chiral-related circular dichroism spectra, DNA hybridization does not produce significant changes in optical signals, thus an optical label is generally needed for sequence-specific DNA detection with optical means. During the last two decades, we have witnessed explosive progress in the area of optical DNA detection, especially with the help of simultaneously rapidly developed nanomaterials. In this chapter, we will summarize recent advances in optical DNA detection including colorimetric, fluorescent, luminescent, surface plasmon resonance (SPR) and Raman scattering assays. Challenges and problems remained to be addressed are also discussed.

6.1 Introduction

Optical detection has long been a powerful tool for biomedical applications. Optical sensors based on bio-recognition events possess some unique advantages over other analytical methods. To name a few, light beam produces much less interference to biological events compared with electronic, electrochemical or magnetic signal sources. Optical signals are immune to electromagnetic interference, capable of

D. Li • C. Fan (✉)
Laboratory of Physical Biology, Shanghai Institute of Applied Physics, Chinese Academy of Sciences, Shanghai 201800, China
e-mail: lidi@sinap.ac.cn; fchh@sinap.ac.cn

G. Spoto and R. Corradini (eds.), *Detection of Non-Amplified Genomic DNA*, Soft and Biological Matter, DOI 10.1007/978-94-007-1226-3_6,

performing remote sensing and providing multiplexed detection within a single device. Optical labels are safe and ease of manipulation compared with classical radioactive labels.

The basic principle of DNA optical sensor is to generate a recordable optical signal upon sequence-specific hybridization. While a few excellent reviews have given comprehensive summarize of the history and updated process of DNA sensors and DNA microarrays [1–7], we will focus on some recent advances on optical detection of non-amplified genomic DNA in this chapter. In the end, we will present a brief outlook for questions remained to be addressed and future potential for these optical DNA sensors.

6.2 Optical Methods for DNA Analysis

6.2.1 Colorimetric Assays for Nucleic Acid Detection Using Au Nanoparticles

Colorimetric biosensors, which mean a detection method based on the color change induced by a bio-recognition event, are particularly impressive since they minimize or eliminate the necessity of using expensive and complicated instruments, sometimes the detection can even be realized by unaided naked eyes.

The milestone work was the development of colorimetric DNA sensor using Au nanoparticles (AuNPs) from Mirkin's group in 1996, which in a sense opens the era of bionanotechnology [8, 9]. Herein we first provide a short description of the interesting optical propertiesy of AuNPs in order to better understand the principle of AuNPs-based colorimetric DNA sensor. AuNPs, or Au colloid has a long history that could date back to at least to the fourth century AD when it was used to stain the Lycurgus cup owing to its brilliant wine color [7, 10]. But correlation of the color of Au colloidal with its small size was first was heralded by Michael Faraday in 1857 in a lecture entitled "Experimental Relations of Gold (and other Metals) to Light" [11]. We must pay a tribute to his insight, even 150 years ago, he noted, "The state of division of these particles must be extreme; they have not as yet been seen by any power of the microscope". The explosion of nanotechnology in the last two decades has confirmed that Au colloids prepared by Faraday were actually spherical AuNPs with a diameter of 10–100 nm. The intense red color of AuNPs is due to the interaction of incident light with a collective oscillation of free electrons in the particles known as localized surface plasmon resonance. When AuNPs aggregate, color of AuNPs changed from red to blue, which was attributed to the interaction of interacting particle surface plasmons and aggregate scattering properties. This simple red-to-blue color change has motivated scientists to design colorimetric sensing strategies by utilizing the analyte-induced AuNPs aggregation. For example, AuNPs loaded with antibodies or antigens has been used in commercialized test strips for HIV or pregnancy testing.

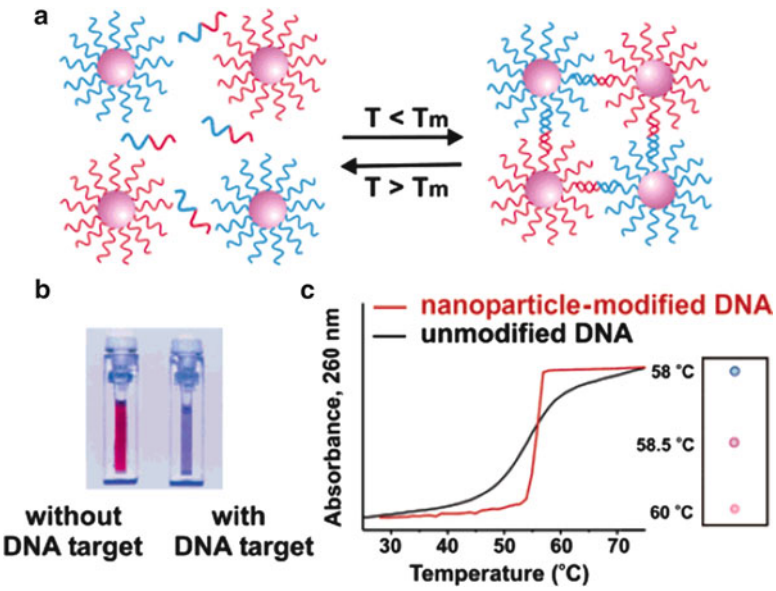

Fig. 6.1 Upon hybridization with the complementary target DNA, probe DNA -functionalized AuNPs will aggregate (**a**), resulting in a *red*-to-*blue* color change (**b**). The aggregation process is accompanied by a sharp increase of the absorbance in the melting profile as compared with regularly DNA hybridization in solution phase (**c**) (Reproduced with permission from Ref. [7]. Copyright (2007) American Chemical Society)

Mirkin's group pioneered the use of aggregation-induced color change of AuNPs in nucleic acid detection. Briefly, AuNPs of 13 nm in diameter was modified with thiolated-probe DNA via Au-S chemistry. Thus upon the addition of target DNA that cross-linked the probe DNA-modified AuNPs through sequence-specific hybridization, a red-to-purple color change is therefore observed. More interestingly, given the nature of DNA hybridization is reversible depending temperature, the aggregation process is reversible; denaturation of the hybridized DNA duplex at elevated temperature (above the melting temperature, Tm) causes the dissociation of aggregates into dispersed AuNPs (Fig. 6.1). Further studies indicated that the melting profiles of the nanoparticle-labeled DNA aggregates were extraordinarily sharp, occurring over a temperature range much narrower than the transition for unlabeled or conventional fluorophore-labeled DNA [12, 13]. By elaborate optimization of influence factors such as AuNPs size, densities of probe DNA on AuNPs and salt concentrations, this colorimetric assay enables the detection of target DNA with a limit of detection (LOD) down to nM.

This simple colorimetric technique offered several advantages for quantitative analysis of nucleic acids: (1) AuNPs is ease of conjugation with thiolated probe DNA. The large surface area of nanomaterials ensures a spherical AuNPs of 13 nm load hundreds of capture probe DNA, meanwhile the three dimensional

(3D) assembly of probe with AuNPs lowers the steric hindrance and favors target-probe hybridization; (2) AuNPs possesses extremely high extinction coefficients (e.g., 2.7×10^8 M^{-1} cm^{-1} at ~520 nm for 13 nm spherical AuNPs, ca. 1,000 times higher than those of organic dyes) [14], thus slight aggregation may result in intense color, suggesting relatively high sensitivity; (3) The simple red-to-blue color change readout does not require expensive, sophisticated instrumentation; (4) last but not least, the sharp absorbance changes in Tm profile could be utilized to discriminate between perfectly matched target oligonucleotides and targets with single base-pair mismatches, holding huge promise in single nucleotide polymorphisms (SNPs) analysis. Therefore, ever since first developed by Mirkin and co-workers, this platform has been increasingly applied for the detection of a wide spectrum of analytes ranging from nucleic acids to proteins, saccharides, small molecules, metal ions, and even cells. It is quickly becoming an important alternative detection tool, holding great potential in clinical diagnostics, drug discovery and environmental contaminant analysis [15, 16].

In addition to this target nucleic acid-induced cross-linking aggregations, Rothberg and Li have proposed an alternative colorimetric method using unmodified citrate-reduced AuNPs in 2003 [17–19]. They found that single-stranded (ss) DNA can be attached on citrate-reduced AuNPs through DNA base-gold interactions and can stabilize AuNPs electrostatically from salt-induced aggregation. In contrast, double stranded (ds-) DNA shows little binding affinity to AuNPs, and, therefore it provides little stabilization against salt. In other words, at an appropriate high salt concentration (e.g., 200 mM of NaCl), citrate-capped AuNPs are stabilized in the presence of ss-DNA, but aggregate in the presence of ds-DNA (Fig. 6.2). This simple phenomenon realized a rapid, label-free sequence-specific detection of target DNA with a LOD also of nM range. Later on, our group further investigated this system and provided a slightly modified mechanism [20–22]. The different affinity of ss- and ds-DNA to AuNPs is attributed to at least three effects. First, DNA bases attach to AuNPs with high affinity via Au-N coordination. Importantly, DNA bases are encapsulated within the negatively charged phosphate backbone of ds-DNA, while they are exposed in ss-DNA. Second, the surface of AuNPs is negatively charged because they are stabilized by citrate ions. Since the charge density of ds-DNA is higher than that of ss-DNA, the electrostatic repulsion between AuNPs and DNA is larger for ds-DNA. Third, ds-DNA is much more rigid than ss-DNA; thus ss-DNA possesses higher freedom to wrap on AuNPs than ds-DNA.

6.2.2 Fluorescent Nucleic Acid Assays

6.2.2.1 Fluorescent Assays Based on Molecular Beacons

Molecular beacons (MB), which were first described in 1996 by Tyagi and Kramer [23], are a class of newly developed probes that are widely used as fluorescent probes. Tyagi and Kramer named this fluorescent DNA probe “molecular beacon”,

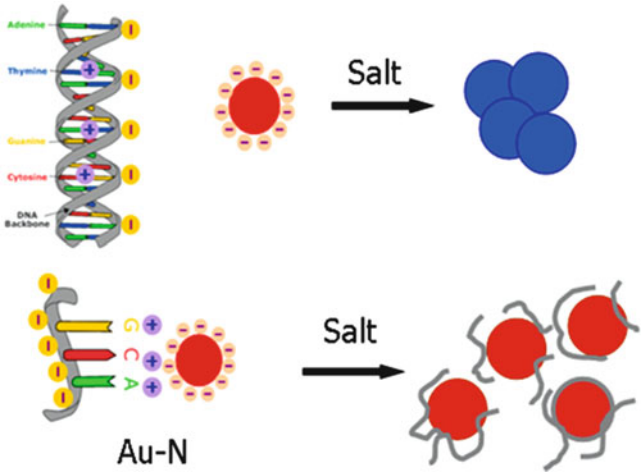

Fig. 6.2 ds- and ss-DNA reveal different affinity of unmodified citrate-reduced negatively-charged AuNPs. ss-DNA possesses higher affinity to AuNPs, it could be attached on AuNPs surface that stabilize AuNPs against salt-induced aggregation, while ds-DNA doesn't

because it emits a light signal upon hybridization with target sequence. Generally, a typical MB is a hairpin structured single stranded oligonucleotide that is modified with a fluorophore and a quencher group at each end of its stem end. The sequence of a MB is composed with two segments including a recognition region of about 15–30 bases flanked by two short complementary stem sequences, which force the entire sequence to form a stem–loop structure at room temperature. In the absence of target DNA, the fluorophore and quencher is forced to be close proximity, where fluorescence is quenched effectively. While in the presence of target DNA that is hybridized with the loop segment of MB, and the resulting duplex structure between target DNA and loop is thermodynamically stable compared with the weaker stem helix, thus the stem-loop structure is forced to open. As a result, the spatial separation of fluorophore and quencher blocks the energy transfer and restores the fluorescence signal (Fig. 6.3a). The application of MBs in DNA sensing was covered by a number of reviews [24–26].

The distinct advantage of MB lies in its ability to real-time monitoring the quantity of target DNA, therefore MB is widely used in RT-PCR to provide a real time measurement of PCR progress [27–29]. In addition to DNA, MB was also employed for real-time quantification of mRNA both *in vitro* and *in vivo* [30, 31]. For example, with the help of confocal fluorescence microscope, MBs could provide a real-time visualization and localization the detection of mRNA in living cells [32].

Despite the variety of applications of MBs in biosensors, the basic principle of detection remains unchanged: the generation of a fluorescent signal is based on hybridization between target oligonucleotides and MBs in a 1:1 stoichiometric ratio. That is, one target oligonucleotide could open only one MB to give fluorescent

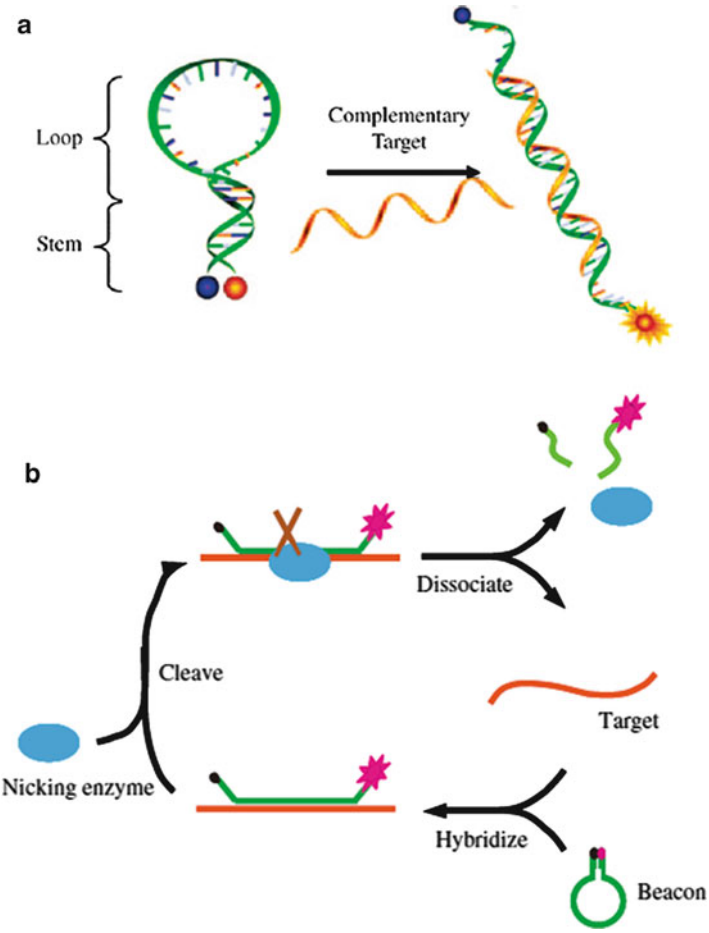

Fig. 6.3 (**a**) Mechanism of a molecular beacon. The MB adopts a stem–loop structure and thus holds the fluorophore (*orange*) and quencher (*blue*) in close proximity. As a result, the fluorescence emission of the fluorophore is strongly suppressed (in the absence of a target). Hybridization with target DNA opens the hairpin structure and recovers the fluorescent signal to allow readout the hybridization event (Reproduced with permission from Ref. [24]. Copyright Wiley-VCH Verlag GmbH & Co. KGaA) (**b**) Working principle of a basic NESA strategy. A nicking enzyme is introduced to cleaves the MB that already be opened by target DNA, resulting dissociation of target from the cleavaged beacon and in turn be released to solution. The as-released target nucleic aid could further hybridize to another beacon and initiate the second cycle of cleavage (Reproduced with permission from Ref. [34]. Copyright (2008) Oxford University Press)

signal. Given the instrument limit of commercial fluorophotometers, MBs could only detect nucleic acids down to nanomolar range.

Recently, a strategy called nicking enzyme signal amplification (NESA) was designed to improve the sensitivity of MB-based fluorescence assay [33–35]. Nicking enzymes are a kind of restriction endonucleases that can recognize a

specific sequence along a double-strand DNA; however, they cleave only one specific strand instead of both strands, leaving a nick in the DNA (Fig. 6.3b). In brief, this strategy introduces a nicking enzyme recognition site in the loop of MB. Upon hybridization with target nuclei acid that yields the duplex recognition domain for nicking enzyme, the nicking enzyme specifically cleaves the MB and this process induces a decreased stability of the two duplexes obtained. Thus target nucleic acid is dissociated from the cleaved beacon and released into solution. The released target nucleic acid could further hybridize to another beacon and initiate the second cycle of cleavage. Eventually, one target nucleic acid could go through many cycles, resulting in cleavage of many beacons. Therefore the limit of detection (LOD) could be significantly pushed down to picomolar range [34].

Despite the three orders of magnitude improvement in sensitivity, the NESA still suffers from one major drawback. It requires the target sequence contains a nicking enzyme recognition site, thus is not appropriate for detection of target with random sequences. Several extended visions of NESA strategy were designed for random sequence detection. For example, Xie and co-workers coupled rolling circle amplification (RCA) with NESA that further improves the LOD down to 85 fM [34]. More recently, Zhou and co-workers [36] presented another modified version of NESA named cascade enzymatic signal amplification (CESA), which they integrated a invasive signal amplification with NESA. Unlike RCA that requires a e padlock probe DNA to capture target nucleic acid, invasive signal amplification does not rely on specific recognition sequences but on a specific structure formed by the specific binding of an upstream probe and a downstream probe to a target DNA; so any target sequence can be detected.

A further improved LOD of 1 fM was achieved in this strategy. In addition to nicking enzyme, sequence-independent exo-exonuclease III and DNA polymerase were also used to digest MBs that “recycles” target nucleic acid to improve the sensitivity [37]. The coupling of MBs with enzymatic digestion cycling possesses great potential for ultrasensitive detection, real-time imaging and location of nucleic acid in-vivo.

6.2.2.2 Fluorescent Assays Based on Nanomaterials

Organic Dye Fluorophores Incorporated in Nano-Scale Matrix

While organic dyes have to be powerful fluorescent labels in bio-diagnostics, they also suffer from intrinsic drawbacks, for instance, limited sensitivity and photo-stability. Moreover, most organic dyes present a certain level of toxicity that hinders their application in vivo cellular studies and imaging. To overcome these disadvantages, researchers attempted to incorporate dyes inside silica NPs [38], which provide an effective barrier keeping the dye from the surrounding environment, both photobleaching and photodegradation phenomena that often affect conventional dyes can be minimized. Using appropriate synthetic conditions, a large number of dye molecules can be incorporated inside a single silica particle

(there can be tens of thousands of dye molecules). Even though there remain some fluorescence quenching phenomena within an NP with a large amount of dye incorporated in a small volume, the goal of obtaining a particle with brighter luminescence is largely successful. Dye-doped NPs produce a highly amplified optical signal compared with a single dye molecule.

Tan's group has pioneered the application of this dye-doped Silica NPs in nucleic acid detection and imagining [39]. They first attached a capture probe DNA on a dye-doped Silica NPs via biotin-avidin interactions. The dye-doped Silica NPs modified capture probe was further used in a sandwich-type fluorescent DNA assay [40]. Hybridization of target DNA with the capture probe brings the dye-doped silica NP to the surface. This provides a large number of dye molecules on the surface for signaling. By monitoring the luminescent intensity from the surface-bound NPs, DNA target molecules can be detected with increased sensitivity (as low as 0.8 pM). The protocol could be also used in array-based multiple DNA analysis and imaging by using different dye-doped Silica NPs. Zhou et al. [41] prepared a class of dye-doped core-shell NPs by attaching thiolated DNA probes to the surface of AuNPs. The AuNPs were then coated with a 10–15 nm silica layer through the (3-mercaptopropyl)trimethoxysilane (MPTS). Two-color DNA microarray-based detection and imaging was demonstrated using Cy3- and Cy5-doped NPs in sandwich hybridization.

Fluorescent Nanomaterials

Quantum dots (QDs) are a class of II-IV or III-V semiconductor nanoparticles with a size scale approximately less than 10 nm [42, 43]. The distinct optical property of QDs is the size-dependent fluorescence properties. QDs possess narrow size-tunable fluorescence spectra with narrow full width-at-half-maxima. The absorption spectra of QDs are broad. The combination of broad absorption spectra and narrow symmetric emission spectra enables QDs attractive for multiplex targets sensing [44]. Meanwhile, QDs have higher quantum yields and are more robust against photobleaching compared with organic dyes, thus also great attention was given to its application in imaging [45].

The size-tunable fluorescence emission and simultaneous excitation feature of QDs render them as ideal fluorophores for wavelength-and-intensity multiple labeling. About a decade ago, Nie and co-workers pioneered the use of QDs embedded beads for multiple DNA detection [46]. The principle of multiplexed optical coding is based on multicolor QDs embedded in polymer beads. The polymer beads were modified with DNA probes. Target DNA was directly labeled with a fluorescent dye. Fluorescence spectra of the single-bead level yield both the coding and the target signals. The coding signals identify the DNA sequence, whereas the target signal indicates the presence and the abundance of that sequence (Fig. 6.4).

In addition to direct labeling, QDs is mainly used as electron donor in fluorescence DNA assays. FRET (or Förster resonance energy transfer) is a through space

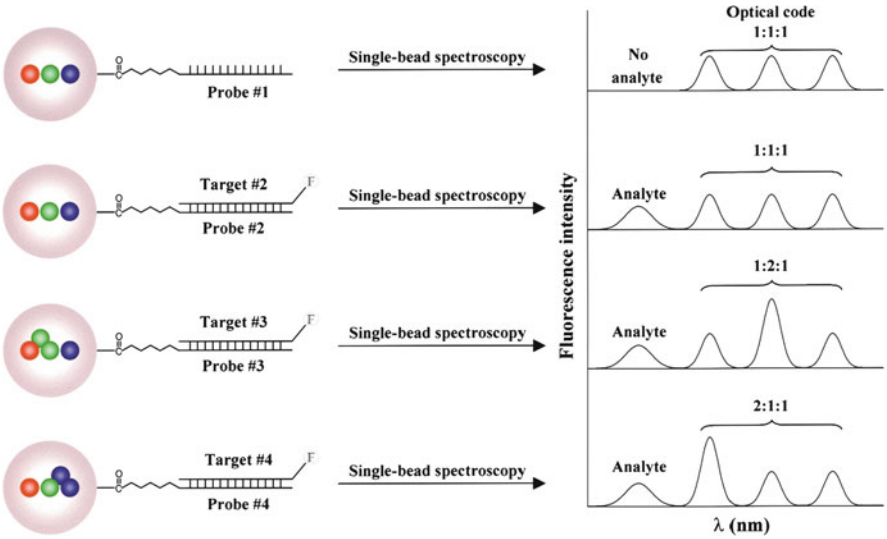

Fig. 6.4 Schematic illustration of DNA hybridization assays using QD-tagged beads. Multicolor optical coding for DNA could be achieved by embedding different-sized QDs into polymeric microbeads at precisely controlled ratios (Reproduced with permission from Ref. [46]. Copyright (2001) Nature Publishing Group)

dipolar coupling interaction that allows electronic energy to be transferred from a donor to an acceptor [47, 48]. The rate of energy transfer depends on the distance between the donor and the acceptor, their relative orientations, and the spectral overlap. The fluorescence emission of QDs has a spectra overlap with the excitation of regular organic dyes. Therefore by careful arrangement of their distance from DNA and of their orientation, FRET may be observed between QDs and dyes.

A typical FRET sensor for nucleic acid, involves a probe DNA attached on a QDs surface. Then a dye labeled target DNA is hybridized with the immobilized probe DNA. As a result, the target DNA brings the fluorophore in close proximity of QDs enough to raise FRET. Several FRET-based sensing strategies for nucleic acids were proposed in the last decades (Fig. 6.5). For example, Ozkan and co-workers modified a CdSe/ZnS QDs with a stem-loop structured probe DNA with an organic quencher 4-(4′-dimethylaminophenylazo) benzoic acid (DABCYL) conjugated at one end of the stem (Fig. 6.5a). In the closed state, the fluorescence of QDs was quenched by DABCYL. In the presence of target that complementary to the loop segment of the probe DNA, DABCYL was brought away from QDs, resulting recovery of fluorescence from QDs [49]. Krull's group designed a strategy to simultaneously detect two target nucleic acid sequences using FRET (Fig. 6.5b) [50]. These two targets were labeled with Cy3 and Alexa Fluor 647, respectively. Probe sequences complementary to these labeled targets were paired with a green QDs and a red QDs. Upon probe–target hybridization, the induced donor-acceptor proximity resulted in FRET-sensitized acceptor fluorescence.

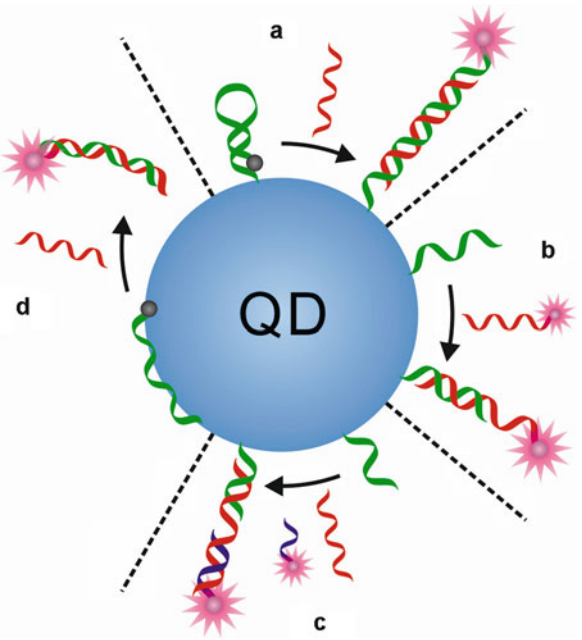

Fig. 6.5 FRET-based sensing strategy for nucleic acids using QDs as donors: (**a**) a QD-based molecular beacon (Ref. [49]); (**b**) hybridization assay for DNA (Ref. [50]); (**c**) a sandwich assay for DNA (Ref. [51]); (**d**) cationic polymer linked QDs and DNA (Ref. [52])

Wang and co-workers have raised a sandwich-typed FRET assay for DNA (Fig. 6.5c) [51]. A streptavidin-coated CdSe/ZnS QDs with emission at 605 nm was paired with Cy5 as an acceptor. The sandwich was constructed with a biotinylated probe DNA complementary to half of target sequence and a Cy5-labeled probe complementary to the other half of target. The strong biotin–streptavidin binding interaction brought the sandwich to the surface of the QD. FRET between QD donor and Cy5 acceptor was observed. Travas-Sejdic employed a cationic polymer as a linker to electrostatically link a dye-labeled probe DNA and QDs (Fig. 6.5d) [52]. The differential interaction of ss- and ds-DNA with $CdTe^{+}$ results in differential changes of FRET efficiency, which was used to recognize the hybridization event.

Besides II-IV semiconductor nanoparticles QDs, Silicon nanoparticlesor nanowires are another class of fluorescence QDs. While bulk silicon is not fluorescent, silicon at nanoscale could generate intense room temperature photoluminescence, which is generally believed to result from a combination of quantum confinement effects. Although of quantum yield (QY) of silicon-based QDs is relatively low (<10 %), they still possesses some unique superiority over II-IV semiconductor nanoparticles QDs in bio-labeling and imaging. For example, the potential toxicity problem of the II-VI QDs associated with release of heavy metal ions (e.g. Cd ions) has not yet been fully addressed, which limits their widespread biological and medical applications [50, 53]. Nontoxic silicon-based QDs reveal the potential as promising candidates. Intense exploration has been done to improve the QY of silicon QDs to facilitate their applications in bio-labeling.

Kortshagen and co-workers recently reported successful preparation of SiQDs with remarkably high ensemble quantum yields exceeding 60 % by using plasma-assisted synthesis with strict removal of oxygen and elaborate surface passivation [54]. Especially, we and our collaborators recently developed a new class of fluorescent silicon nanospheres (SiNSs), each containing several hundreds of SiQDs [55, 56]. The as-prepared nanospheres possess excellent aqueous dispersibility, strong fluorescence (quantum yield: >15 %), robust photo-stability and favorable biocompatibility. Nevertheless the process of synthesis SiQDs with higher QYs, their application in DNA detection assay is still far behind that of QDs, and we believe that this is a promising field for future research.

In addition to QDs, up-converting rare-earth nanophosphors (UCNPs) are another class of fluorescence nanoparticles [57]. In contrast to QDs that adsorb UV light and emit visible light, UCNPs adsorb low energy light, usually near-infrared (NIR) or infrared (IR), and emit high energy light (UV or visible) through multi photon absorptions or energy transfers. UCNPs consist of rare earth atoms that are embedded in a crystalline host matrix. Among the varies of up converting materials, NaYF4 nanocrystals are reported as the most effective host for infrared-to-visible up conversion when doped with Er or Yb ions [58]. Although the quantum yield of UCNPs is not even comparable with QDs, is still possesses some unparalleled advantages in bio-labeling applications. For example, the noninvasive and deep penetration of NIR radiation could realize deep tissue imaging. Meanwhile, since the background fluorescence of living organisms could not be excited by NIR light, UCNPs labeling provides unmatched sharp contrast in imaging.

The bottle-neck of UCNPs in nucleic acid assay comes from the tough conjugation of DNA with UCNPs. Despite recent advances in synthesis of UCNPs with controllable size and shape, the as-synthesized UCNPs are usually coated with hydrophobic organic ligands and suffer from poor water-solubility. Currently, several surface modification strategies have been proposed to enable UCNPs water-soluble and conjugate with oligonucleotides. One general strategy to convert hydrophobic nanoparticles water soluble is to encapsulate with silica or amphiphilic copolymers [59]. For example, Tanke's group has coated Y2O2S:Er UCNPs with silica, which was then conjugated with biotin [60]. This biotinylated-UCNPS were successfully employed as fluorescence reported in nucleic acid arrays. Compared with Cy5 label, the assays with UCNPs reveals four times improved sensitivity. Another versatile strategy for synthesizing water-soluble and carboxylic acid-functionalized UCNPs was performed by directly oxidizing oleic acid ligand to azelaic acid ($HOOC(CH_2)_7COOH$) with the Lemieux-von Rudloff reagent. The free carboxylic acid groups on their surface enable further conjugation with DNA probes [61]. By using this protocol, Huang and co-workers modified UCNPs with a DNA capture probe and constructed a sandwich-type DNA assay including a reporter dye-labeled DNA on UCNPs. Upon illumination of the UCNPs with NIR light, the visible emission light of UCNPs could be adsorbed by the dye, producing FRET from UCNPs to dye; the fluorescence of the dye could be observed as the readout of this UCNPs-based DNA assay.

Nanomaterials as Fluorescence Quenchers

Fluorescent detection methods are still the most employed in nucleic acid assay due to the commercial availability of a wide spectrum of fluorophores, the ease of fluorescent labeling, and the inherent capability for real-time detection. While fluorescent detection is usually highly sensitive, the detection sensitivity is often limited by the presence of background emission. While organic quenchers have proven their utility, they suffer from relatively low quenching efficiency, and, more importantly, quenching efficiencies often vary significantly from one dye to another.

Interestingly, some metallic or carbon nanomaterials have shown ultrahigh fluorescence quenching ability. For example, the quenching mechanism of metal clusters has been well theoretically studied and proven to be a resonant energy transfer process [62–64]. Meanwhile, AuNPs have a Stern–Volmer quenching constant (KSV) that is greater with several (>5) orders of magnitude than that of typical small molecule dye quencher pairs [65]. This "super-quenching" ability of AuNPs has found great implications in fluorescence-based nucleic acid assays that great suppress the background. Dubertret et al. designed an AuNPs-based nanobeacon that replaced organic quenchers with 1.4-nm AuNPs, and found that AuNPs served as a universal quencher that could quench a range of fluorophores with 100-fold higher quenching efficiency than organic quenchers [66]. This so called "nanobeacon" not only led to improved sensitivity but also remarkably high selectivity for single-base mismatch discrimination. Nie and coworkers later reported a stem-less probe on 2.5-nm AuNPs that still demonstrated target-induced conformational change and fluorescence variation in response to the binding of target DNA [67]. Although these small-sized AuNPs revealed decent performance as effective quenchers in nanobeacon, their crowded surface could only accommodate one or several oligonucleotides probes. Recently, we employed larger-sized AuNPs of 15 nm in diameter to construct multicolor nanobeacons [68]. Importantly, it is possible to anchor many DNA probes at one single particle due to the increased surface area. As a proof-of-concept experiment, three DNA probes designed for three tumor-suppressor genes were immobilized at the AuNPs surface, each carrying a unique fluorophore. This nanobeacon exhibited rapid hybridization kinetics (minutes), and could respond specifically to different gene targets (Fig. 6.6). The organic dye in the nanobeacon could also be replaced by fluorescent QDs [15, 69], providing new opportunities for nanobeacons incorporating multiple functional nanoparticles.

In addition to metallic nanoparticles, some carbon nanomaterials including one dimensional (1D) single-walled carbon nanotubes (SWNTs) and two dimensional (2D) graphene have been observed to interact differentially with ss- and ds-DNA, which also enables them to be used as effective quenchers in fluorescence DNA detection. To take SWNTs as an example, ss-DNA has been demonstrated to interact noncovalently with SWNTs [70, 71]. In detail, ss-DNA molecules could wrap around SWNTs by means of π-stacking interactions between the nucleotide bases and the sidewalls of individual SWNT, resulting stable complexes, while for dsDNA, the affinity is significantly weaker. This difference in the binding

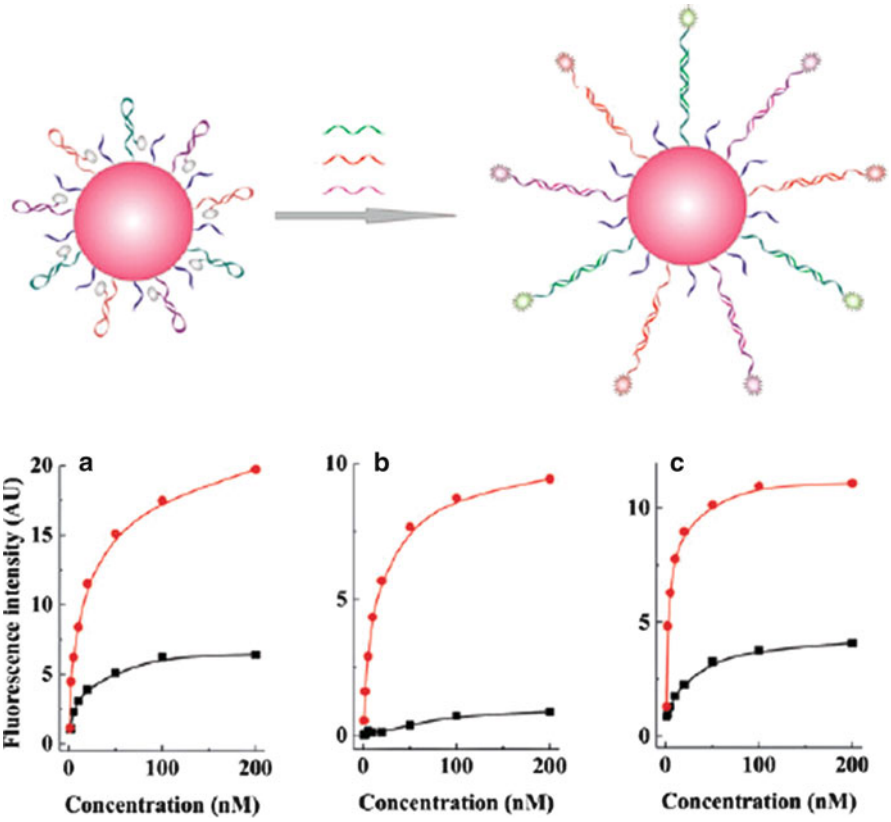

Fig. 6.6 Multicolor nanobeacons for multiplexing detection of three different cancer DNA markers. The multicolor nanobeacons are hybridized with three perfectly matched targets and three single mismatched targets, showing high sequence specificity that arises from the conformational constraint (Reproduced with permission from Ref. [68]. Copyright Wiley-VCH Verlag GmbH & Co. KGaA)

interactions of SWNTs with ssDNA and dsDNA has provided the basis for their use to report DNA hybridization. Plus, SWNTs was found as an effective quencher to quench fluorophores nearby. This quenching was found to be quite universal to a variety of fluorophores, as well as QDs, and it is thought that either energy transfer or electron transfer might contribute to such high quenching efficiency [72, 73].

Tan and Yang combined the super quenching feature of SWNTs together with its' ability to differentiate ss- and ds-DNA, and designed a SWNTs-based strategy for DNA sensing [74]. They demonstrated that fluorophore-labeled DNA probes were efficiently quenched in the presence of SWNTs while they were released from SWNTs upon hybridization, leading to fluorescence recovery [74, 75]. This strategy, however, needs a fluorophore-tagged ss-DNA probe, which increases the detection cost. They also moved one-step further to introduce a DNA intercalating

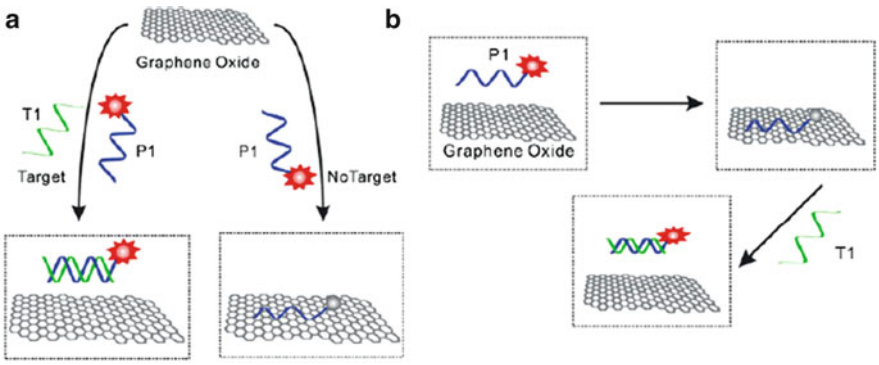

Fig. 6.7 (**a**) Scheme for the fluorescent DNA detection based on the ss-DNA/ds-DNA discrimination ability of GO. (**b**) Scheme for the target hybridization-induced probe liberation from GO (Reproduced with permission from Ref. [80]. Copyright © 2011 WILEY-VCH Verlag GmbH & Co. KGaA, Weinheim)

dye ethidium bromide (EB) to replace fluorophore and developed a cost-effective label free method for fluorescence DNA detection [76].

As a planar molecule, ethidium bromide can absorb on the sidewall of SWNTs. A mixture of the dye, the capturing ssDNA, and SWNTs formed a self-assembly of three components, generating complete quenching of fluorescence. After the introduction of target DNA, ds-DNA formed between the capturing DNA and the target. The adsorbed ethidium bromide preferred to intercalate into the hybridized bases, which disturbed the interaction of the dye and SWNTs, resulting in fluorescence recovery.

Graphene is a single layer of carbon atoms in a closely packed honeycomb two-dimensional lattice [77, 78]. Recently, graphene was also found to be an excellent super fluorescence quencher, however, different from SWNTs, the quenching mechanism of graphene was theoretically and experimentally attributed to be only long-range resonance energy transfer [64, 79]. We carried out molecular dynamics (MD) simulation to describe the interaction of graphene oxide (GO) with ss- and ds-DNA, which indicated that ss-DNA adsorbed strongly to graphene oxide (GO) sheets while ds-DNA did not [80]. Thus, similar to SWNTs, Lu et al. employed GO to adsorb and quench dye-labeled DNA probes, which could be liberated upon hybridization, leading to fluorescence increment [81]. He et al. designed a new approach that relied on different binding kinetic of ss-DNA and ds-DNA to GO, which led to sequence-specific detection with high sensitivity and rapid response time (<5 min) [50]. More significantly, due to the availability of large planar surface of GO, multicolor DNA detection was realized by using differentially labeled DNA probes (Fig. 6.7). Another unparalleled advantage of carbon nanomaterials, is their ability to cross cell membrane [82, 83]. Thus, in vivo analysis or imaging nucleic acid is highly anticipated [64, 84].

6.2.3 *Chemiluminescent and Electro-Generated Chemiluminescent DNA Assay*

6.2.3.1 Chemiluminescent DNA Assay

Luminescence is the emission of light without heat, and more specially the generation of light from chemical reactions (chemiluminescence, CL). This long history of CL has been summarized in a few review articles [85–87]. Since excitation light is not required for sample radiation, problems frequently encountered in fluorescence, such as light scattering, source instability and high backgrounds due to unselective photoexcitation are absent in CL assay. Consequently, CL has found great advantages in biodiagnostics [88].

In a typical CL reaction, an organic dye, which is not luminescent in the ground state, was oxidized by a strong oxidizing agent in the presence of a catalyst (chemical or biological). The most commonly used dye is luminol, while oxidation of luminol with hydrogen peroxide (oxidizing agent) in the presence of a catalyst results in the conversion of the ground state of luminol into an activated state (chemically induced electronic excited states). A strong blue emission (at 450 nm wavelength) can be observed as a result of the decay of the excited states back to the ground state [89]. The most intensively used catalysts that enhance the CL of luminol is horseradish peroxidase (HRP). The mechanism of HRP enhanced CL has been extensively studied [86], suggesting HRP reacts with H_2O_2 to form an oxidized HRP (HRP I) that reacts with the anion of luminol to form a half reduced enzyme (HRP II) and a radical of luminol. The enzyme returns to the reduced form (HRP) by reaction with a second molecule of luminol. The catalytic phenols form preferentially phenoxy radicals in contact with horseradish peroxidase and act as electron-transfer mediators to increase the efficiency of luminol radical formation. However, the luminol-based CL assay is mainly applied to immunoassays instead of DNA detection, which was attributed to the poor sensitivity. In the early phase of luminol-based DNA assay, luminol was directly conjugated with DNA as reporter probe in a sandwich-typed CL assay. A luminol derivative, N-(4-aminobutyl)-N-etylisoluminol (ABEI) is the only tracer used in immunoassay. However, luminol is more efficient in its free state. Upon conjugation with DNA, it lost most of CL properties; thereby this ABEI-tagged CL assay did not reveal satisfied performance. An alternative protocol is to use HRP as an enzyme label in sandwich-typed DNA assay and luminol-H_2O_2 mixture was added to generate CL signal and report the hybridization event, however, which is also found limited success.

In addition to HRP, some other catalysts, including Co^{2+} [90], Cu^{2+} [91, 92], or AuNPs [93, 94] could also enhance the CL of luminol-H_2O_2 system, although the detailed mechanism is not completely clear yet. Among these enhancers, AuNPs has found widely implications in CL DNA assay owing to the ease conjugation of DNA with AuNPs. For example, Willner's group reported that horseradish peroxidase-like DNAzyme-functionalized AuNPs could act as catalytic labels for the amplified detection of DNA with a LOD of 0.1 nM [93]. Li and co-workers demonstrated a

sandwich-typed CL assay for DNA detection using tadpole-shaped AuNPs [94]. Zhang and co-workers found that Au nanoaggregates induced by salt possesses higher enhancement towards the CL of luminol-H_2O_2 than AuNPs [95]. The Au nanoaggregates were used as catalyst in a CL DNA assay and a LOD of 1.1 fM was achieved.

Historically, the CL of luminol system has been preceded by a more sensitive dye of acridinium. Interaction of an acridinium ester (AE) with an alkaline hydrogen peroxide solution would trigger a short flash of light at 430 nm within 5 s or less. Nelson's group have synthesized a number of derivatives of this AE and characterized their chemiluminescent properties [96]. These derivatives display significant differences in the kinetics of the chemiluminescence reaction as well as optimal pH for light production. The first acridinium derivative of practical use was 4-(2-succinimidyl-oxycarbonylethyl)-phenyl-10-methyl-acridinium-9- carboxylate (AE-NHS). AE-NHS does not show the best quantum yield and is not very stable especially at room temperature although its stability is increased after coupling. More efficient compounds are found in thiol, sulphonamide, hydroxamic, oxime and chloroxime series [86]. After covalent conjugation to DNA helix, acridinium labels show increased stability toward hydrolysis. These property enables AE-derivatives to be used in important applications in Chemiluminescence DNA assay, including simultaneous detection of *gag* and *pol* regions of HIV [97] and discrimination of the single-base mismatch between wild-type and mutant sequences corresponding to the reverse transcriptase coding region of HIV-1 [98].

6.2.3.2 Electro-Generated Chemiluminescent Assay

Electro-generated chemiluminescence, or electrochemiluminescence (ECL) is an analogue of CL. ECL is chemiluminescence triggered by electrochemical techniques that undergoes a high-energy electron transfer reaction to generate an excited state. The combination of electrochemistry with chemiluminescence, has proven to be a powerful analytical tool [99, 100]. For example, in the classical ECL of tris(2,2′-bipyridyl) ruthenium $(Ru(bpy)_3)^{2+}$ that was developed by Bard [101], its ECL mechanism has been well-illustrated. $(Ru(bpy)_3)^{2+}$ ECL reaction occurs by oxidizing $(Ru(bpy)_3)^{2+}$ to produce$(Ru(bpy)_3)^{2+*}$ in the presence of a strong reducing agent. The most commonly used reducing agent for this type of ECL reaction is tripropylamine (TPrA). This mechanism is termed the oxidative-reduction mode [102, 103]. It has been proposed that its oxidative-reduction ECL mechanism is as follows:

$$(Ru(bpy)_3)^{2+} - e^- \rightarrow (Ru(bpy)_3)^{3+} \tag{6.1}$$

$$TprA - e^- \rightarrow TprA^{\bullet +} \tag{6.2}$$

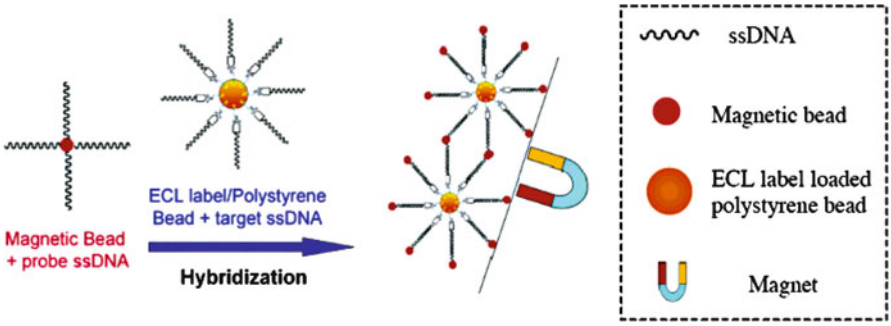

Fig. 6.8 Schematic diagram of DNA hybridization on a polystyrene bead as the ECL label carrier and a magnetic bead for the separation of analyte-contained ECL label/polystyrene beads (Reproduced with permission from Ref. [106]. Copyright (2004) American Chemical Society)

$$\mathrm{TprA}^{\bullet+} \rightarrow \mathrm{TprA}^{\bullet} + \mathrm{H}^{+} \tag{6.3}$$

$$(\mathrm{Ru(bpy)_3})^{3+} + \mathrm{TprA}^{\bullet} \rightarrow (\mathrm{Ru(bpy)_3})^{2+*} + \text{products} \tag{6.4}$$

$$(\mathrm{Ru(bpy)_3})^{2+*} \rightarrow (\mathrm{Ru(bpy)_3})^{2+} + \mathrm{h}\nu \tag{6.5}$$

The distinct advantage of ECL is its high sensitivity. $Ru(bpy)_3^{2+}$ can be highly sensitively detected at subpicomolar concentrations with an extremely wide dynamic range of greater than six orders of magnitude. Consequently, this super high sensitivity of ECL has found great implications in DNA sensors. The application of ECL in DNA assay was summarized in an excellent review [104].

This field was pioneered by Bard's group in 1995 [105], lately they integrated ECL with magnetic concentration to further improve the sensitivity [106]. In their protocol (Fig. 6.8), $Ru(bpy)_3^{2+}$ label was encapsulated in polystyrene (PS) beads. The advantage of PS beads is that one PS bead could carry up to 7.5×10^9 molecules of $Ru(bpy)_3^{2+}$. Then biotinylated target DNA was modified on the surface of these $Ru(bpy)_3^{2+}$ loaded PS beads via biotin-avidin interaction. The target DNA was complementary to a probe DNA that was modified on a magnetic beads surface. Upon addition of a magnetic field, the target DNA-PS beads containing $Ru(bpy)_3^{2+}$ were magnetically separated and transferred into an acetonitrile solution where the polystyrene beads dissolve the ECL label is released. This is followed by ECL detection and a LOD of 1 fM was achieved.

In addition to these solution phase ECL assays, solid state ECL DNA assays were also developed. The first model assay was also proposed by Bard's group [107]. In brief, they first modified a Au(111) electrode with a capture probe DNA. Upon hybridization with target DNA carrying a $Ru(bpy)_3^{2+}$ ECL label, $Ru(bpy)_3^{2+}$ was brought to the surface of electrodes and generated ECL signal. This simple method, however, requires the covalent modification of target DNA

with $Ru(bpy)_3^{2+}$, which is actually inappropriate for clinical diagnostics. Thereby, some sandwich-typed hybridization assays were further developed [108, 109]. An alternative type of hybridization assay was presented by Zhang and co-workers by using the conformational change of probe DNA [110]. The modified Au electrode with thiolated hairpin probe DNA was tagged with $Ru(bpy)_3^{2+}$. In the absence of target ss-DNA, the ECL probe immobilized on the surface of the electrode was in its folded configuration, in which its termini were held in close proximity to the electrode, and thus a strong ECL signal could be generated. In the presence of target ss-DNA, a stem-loop of the ECL probe on the electrode was converted into a linear double-helix configuration due to hybridization, resulting in the tag moving away from the electrode surface, which in turn decreased the ECL signal. This method avoids the introduce of a $Ru(bpy)_3^{2+}$-tagged reporter DNA probe; however the "signal-off" detection mode is not a favorite option in sensor design.

In these works, the employed solid state ECL reporter DNA probe carries only one $Ru(bpy)_3^{2+}$ label, thus it produces only one ECL photon for one hybridization event. Motivated by the work of Bard's group in solution phase [107], researchers also employed polymer beads and nanoparticles that load multiple number of $Ru(bpy)_3^{2+}$ as ECL reporters, thereby one hybridization event could correspond to multiple ECL photons, which may improve the sensitivity. For example, AuNPs prepared by the classical citrate-reduced method is negatively charged, thereby AuNPs are "sticked" to aggregates upon interaction of positively charged $Ru(bpy)_3^{2+}$ [111]. The resulted Au nanoaggregates carry a large number of $Ru(bpy)_3^{2+}$, which might be a powerful label for nucleic acid detection. Another example was reported by Zhang and co-workers by using AuNPs [112]. The large surface area of AuNPs enables them to load multiple number, or multiple kind, of biomolecules. For example, one AuNPs of 12 nm in diameter could carry up to a few hundreds of ss-DNA [113]. Zhang et al. modified a thiolated ss-DNA with a $Ru(bpy)_3^{2+}$ at the other terminal, and the $Ru(bpy)_3^{2+}$-functionalized ss-DNA was further covalently attached to AuNPs, thereby one as-prepared AuNP was loaded with hundreds of $Ru(bpy)_3^{2+}$. The resulted DNA-$Ru(bpy)_3^{2+}$-AuNPs was then used as reporter probe in a sandwich-typed ECL DNA assay and a LOD of 5 pM was achieved.

Some DNA intercalators were recently reported as co-reactants for ECL DNA hybridization assays. Park and co-workers found some duplex DNA intercalators including doxorubicin, daunorubicin or 2-phenylindole shows favorable ECL with $Ru(bpy)_3^{2+}$ at +1.19 V (versus Ag/AgCl), while the non-intercalated ssDNA does not [114]. Several pathogens were detected using this ECL approach, and a good specificity of single point mutations for hepatitis disease was obtained by the 2-phenylindole-intercalated $Ru(bpy)_3^{2+}$ ECL.

It should also be noted that a brand-new ECL system using semiconductor QDs was proposed by Ju's group [115–117]. They found that aqueous-soluble CdTe or CdSe QDs show intensive anodic ECL with a peak value at +1.17 V (vs Ag/AgCl) in basic buffer at an indium tin oxide (ITO) electrode. The ECL emission was demonstrated to involve the participation of superoxide ion produced at the ITO surface, which could inject an electron into the 1Se quantum-confined orbital of CdTe to form QDs anions. The collision between these anions and the oxidation

products of QDs led to the formation of the excited state of QDs and ECL emission. Therefore, CdTe QDs could also be employed as ECL labels in DNA assay and a LOD at fM scale was achieved [118].

6.2.4 Surface Plasmon Resonance (SPR) Nucleic Acid Assays

6.2.4.1 SPR Spectroscopy

Surface plasmon resonance (SPR) spectroscopy is a surface analysis method based on changes in the optical reflectivity of a thin metal film (typically gold) when analytes adsorb or bind to its surface or to any material coated onto its surface (see Chap. 9). Surface plasmon (SP) is defined as the plasma oscillations that can propagate at the interface of a metal and a dielectric medium. The electromagnetic field of a SP is confined at the metal–dielectric boundary and decreases exponentially into both media, thereby SP is extremely sensitive to changes in the refractive index of the dielectric. In a typical SPR spectroscopy, a polarized monochromatic light beam is passed through a prism and its attached gold-coated glass slide, and reflected off the thin gold coating, which is in contact with the liquid solution of interest. Excitation of SP at the gold/solution interface results in nearly complete attenuation of the specular reflected light intensity for incident angles very near the SPR angle. The specular reflected light intensity versus angle at fixed wavelength or versus wavelength at fixed angle reflects the refractive index change at the interface.

Ever since the first SPR instrument (BIAcore) was commercialized in 1990 [119, 120], SPR has been a powerful label-free method for real-time monitoring the biomolecular recognition events at surfaces including immunological analysis, studies of protein-protein interaction, molecular-biological studies on the mechanisms of gene expression, signal transduction and cell-cell interactions, the screening of new ligands, the quantification of protein adsorption and immobilization, the evaluation of surfaces for biocompatibility, epitope mapping, the determination of affinity constants, and the examination of the kinetics of binding [121–123]. In addition to quantitatively detection of analytes, one distinct feature of SPR sensor is that it could also monitor the conformational changes of surface-immobilized biomolecules.

The application of SPR in nucleic acid detection was started in the middle of 1990s [124, 125]. The early stage SPR sensors include one capture on the SPR substrate and the complementary target strand in solution. The hybridization of target strand with capture probe resulted changes of SPR angles. Unfortunately, the inability of conventional SPR to measure extremely small changes in refractive index hinders its application in ultrasensitive detection. To address this drawback, several approaches have been developed. Among them, substantial interest has been focused on utilizing external labels to enhance the sensitivity of the current technique. Keating and co-workers introduced sandwich-typed assay and an AuNPs labeled reporter probe [126]. Since the bulk refractive index of AuNPs is significantly higher than that of DNA and the electromagnetic interaction between metallic nanoparticles and metal surfaces may also help influence the plasmon mode

propagation, the introduced AuNPs label significantly amplifies the SPR response. With the help of AuNPs, LOD for a target was improved from 10 nM of regular assay to 10 pM.

6.2.4.2 SPR Microscopy

Recently, another SPR-related technique, SPR microscopy (SPRM), or "SPR imaging" (SPRi), has been developed to provide high-throughput real time information about the amount and distribution of adsorbed molecules at the interfaces with high spatial resolution [121]. The invention of SPR microscopy [127, 128], led the application of SPR to the imaging of biomolecular surface interactions. In principle of taking SPR images is by introducing a parallel light beam for uniform illumination of a surface at a fixed angle and recorded the reflected beam forming the image at a CCD camera. This configuration is sufficient to determine thickness with Angstrom-level resolution.

The thickness-sensitive feature of SPR microscopy enables it to be a powerful tool to study protein-protein, protein-DNA interactions that induce significant surface topography changes [129]. Corn's group has been very active in the development of SPRi-based detection of oligonucleotides [129–131]. In their early work, a single stranded capture probe DNA was first immobilized on SPR substrate. Upon hybridization with target DNA, the SPR image evolved rapidly, resulting in brighter spots, showing the potential of SPRi in DNA detection [130]. However, DNA hybridization does not induce significant changes in the layer height, thus this proof-of-concept label-free method is actually found limited practical success. Later on, the same group further amplified the SPRi response by introducing a sandwich-typed hybridization and a streptavidin-tagged reporter probe to improve the thickness of the DNA layer resulted by target-induced hybridization [132]. The combination of DNA hybridization and streptavidin-biotin binding improved the LOD for DNA hybridization using SPR imaging by a factor of ~4. Interestingly, the SPRi signal could be further improved by multilayers of streptavidin/DNA formed by successively assembly of biotin-labeled target DNA and streptavidin. This in situ monitoring of DNA hybridization, could be easily integrated to 1D arrays, or 2D arrays created by microfluidic techniques, to realize high-throughput nucleic acid analysis [133]. This hybridization event occurred at the SPR substrate, could be cycled by digestion with ExoIII. The enzymatically-assisted SPR imaging process realized a 10^2–10^3 improvement of sensitivity for a 16-mer target ssDNA [134].

6.2.5 Surface-Enhanced Raman Scattering (SERS) in Nucleic Acid Detection

Raman is a vibrational spectroscopic technique to study vibrational, rotational, and other low-frequency modes of molecules. Raman spectrum is obtained from the

inelastic scattering, or Raman scattering, of monochromatic light in the visible, near infrared, or near ultraviolet range. The limit of conventional Raman spectroscopy is its weak intensity, often requiring the use of powerful and costly laser sources for excitation. Interestingly, Raman scattering could be enhanced by factors of up to 10^8 when a compound is adsorbed on or near special metal surface, or 10^{14}–10^{15} when adsorbed on rough coinage metallic (Cu, Ag, Au) nanoparticles surface [135–137]. This phenomenon is called surface-enhanced Raman scarring (SERS). After decades of debate, the mechanism of SERS could be sorted into two classes which were called electromagnetic and chemical, respectively [137]. Briefly, the former focus on the enhanced electromagnetic fields which can be supported on metal surfaces with appropriate morphologies, while the latter on changes in the electronic structure of molecules which occur upon adsorption and which can lead to resonance.

In addition to ultra-high enhancement factor, SERS also possesses other attractive advantages, such as narrow Raman band, and high resistance to interferences of environmental factors (e.g., humidity, oxygen, and foreign species), thereby has been considered as an attractive method for DNA detection [138, 139]. Mirkin and coworkers pioneered the use of SERS for DNA targets detection [140]. They designed a Raman nanoprobe that consists of 13-nm-diameter AuNPs functionalized with Raman dye-labeled oligonucleotides. After Ag staining, the Ag particles can grow around the Cy3-labeled nanoprobes, leading to large Raman scattering enhancements. Thus, they demonstrated that six different oligonucleotide targets could be simultaneously detected with AuNPs labeled with different Raman probes. Significantly, the detection limit was down to 20 fM due to the strong SERS signal intensity. Moskovits and co-workers proposed an alternative SERS-based strategy for DNA detection (Fig. 6.9) [141]. By self-assembling probe-tethered Ag nanoparticles to a smooth Ag film using the complementary target species, they created electromagnetic "hot spots" on smooth Ag surface, which strongly enhance the Raman signal of the species present in the hot spot. Kim and Lee [142] replaced the smooth metal surfaces with rough metal nanowires to further improve the interface roughness and in turn enhancement factor, and demonstrated a nanoparticle-on-nanowire configuration SERS sensor for multiplex pathogen DNA. Very recently, our group proposed an alternative Ag nanoparticle-on-Silicon nanowire SERS platform and found that the in situ grew AgNPs on Silicon nanowires (SiNWs@AgNPs) revealed a SERS enhancement factor of $\sim 10^{10}$ [143]. Then a sandwich-typed DNA assay with A Raman tag was further constructed on the SiNWs@AgNPs substrate (Fig. 6.10). This Ag nanoparticle-on-Silicon nanowire platform revealized a remarkably low LOD of $\sim$1 fM for DNA target. Faulds and Graham also intensively devoted to the design of novel SERS-based DNA sensor [144–146]. One of their representative work is that they prepared a kind of dye-coded, DNA-functionalized silver nanoparticles [147]. Target DNA-induced sequence-specific hybridization produced the assembly of individual nanoparticles to nanoaggregates, which strongly enhanced the SERS signal of surfaces-coated dyes.

In addition to these efforts of bringing SERS tag-loaded nanoparticles to the close proximity of metal (bulk or nano) surfaces with DNA, another type of SERS-based

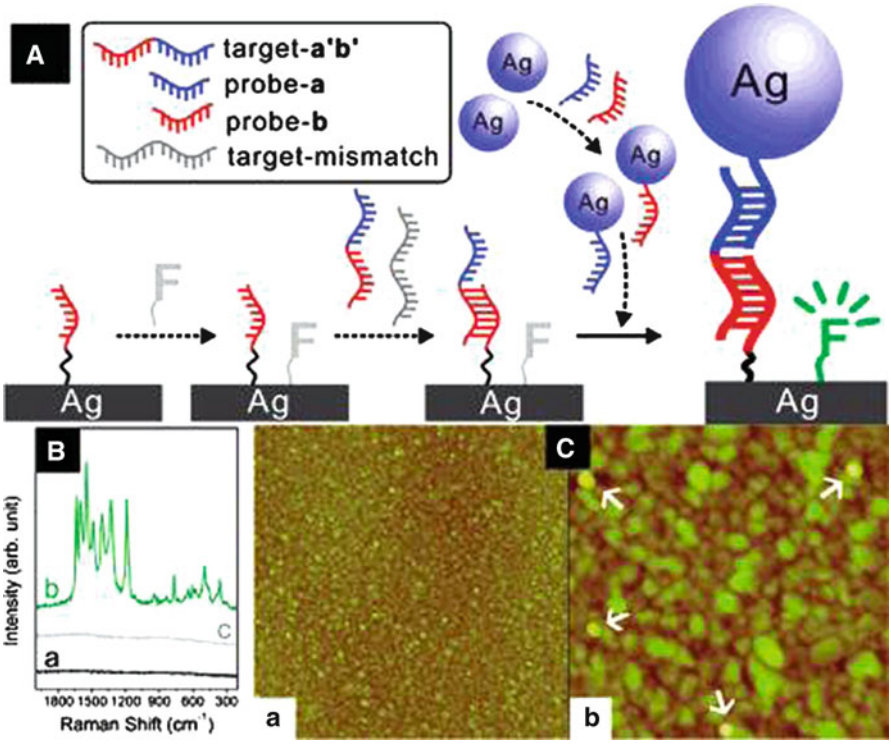

Fig. 6.9 (**A**) Schematic illustration for the detection of ss- DNA by SERS. (**B**) SERS spectra (vertically offset for clarity) indicating the target DNA hybridization-induced enhanced Raman signal. (**C**) Representative AFM images confirming the attachment of AgNPs to Au surfaces by target DNA (Reproduced with permission from Ref. [141]. Copyright (2007) American Chemical Society)

sensor involves the attachment of DNA-labeled SERS tag to the close surface of metal nanoparticles. For example, Vo-Dinh and co-workers [148] represented a plasmonics-based nanoprobe, referred to as a "molecular sentinel" (MS), consisting of a DNA hairpin loop having a Raman label molecule at one end and a metal nanoparticle at the other end. The nanoprobes combines the modulation of the plasmonics effect to change the SERS intensity of the label and the specificity of a DNA hairpin loop sequence to recognize and discriminate a variety of molecular target sequences. Upon hybridization with complementary target sequence that opens the hairpin capture probe, the Raman label was physically removed away from the metal nanoparticle, thus quenching the SERS signal. This "molecular sentinel" strategy was successfully employed for SERS detection o HIV-I virus segment. Johnson and co-workers [149] presented indirect nucleic acid capture strategy to draw SERS tag to the surface of AuNPs with the help of hybridization with target DNA. In their design, a 53-mer West Nile Virus (WNV) genome target DNA was

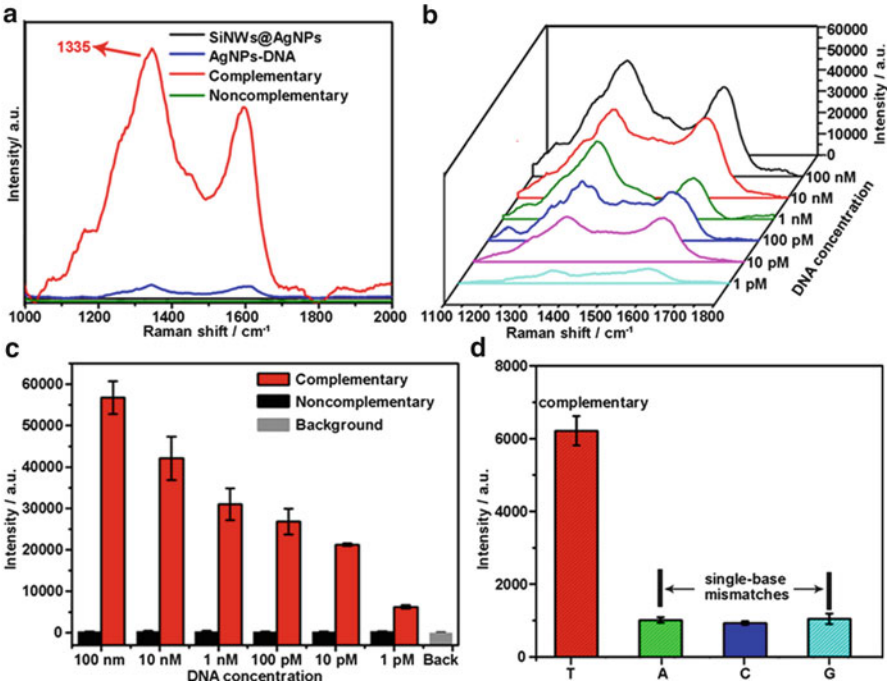

Fig. 6.10 Schematic illustration for the detection of DNA by the SiNWs@AgNPs SERS platform (Reproduced with permission from Ref. [141]. Copyright (2011) Elsevier)

first hybridized in solution with thiolated complementary capture (26-mer) probes and SERS tag-modified reporter (25-mer) oligonucleotide probes, after which the hybridized ternary complex was added to a colloidal suspension of AuNPs and SERS spectra were immediately acquired upon laser excitation.

6.3 Outlook

In this chapter, we have summarized different approaches for optical detection of non-amplified DNA targets. Nanotechnology has shown great advantage in this area. Signal amplification with biomolecular nanoprobes has led to extremely sensitive assays with attomolar detection limit, which represents sensitivity improvement up to six orders of magnitude compared to conventional fluorescent detection (1–10 pM).

Despite such tremendous progress, there remain several challenges for optical DNA detection technologies before they can be widely accepted in clinical or food-related applications. First, DNA hybridization occurring at the nanomaterial surface is inherently low in recognition efficiency and slow in binding kinetics. This is

because the use of inorganic nanomaterials introduces interfaces that bring about the problems of heterogeneous diffusion and convection that are not present in homogenous solution. Second, while some DNA assays have realized ultrahigh sensitivity, they typically require multiple steps that significantly increase the operation complexity. Third, only a few of the mentioned assays show excellent performance in complex biological matrixes (e.g. serum). Thus, non-specific binding is still a major problem that should be studied in order to realize practical applications of these new assay methods.

Notably, the emerging DNA nanotechnology might provide unprecedented opportunities to meet these challenges. For example, the recently developed DNA origami-based chips [150, 151] provide a potentially promising solution to overcome the interface problem since DNA origami structures, in contrast to inorganic nanomaterials, are essentially in aqueous solution. While this method is rather immature in their current form, the combination with high-speed and high throughput readouts as well as automated devices [152], might eventually lead to an unparalleled platform for DNA detection, as well as for the detection of a range of biomolecules.

References

1. Sassolas, A., Leca-Bouvier, B.D., Blum, L.J.: DNA biosensors and microarrays. Chem. Rev. **108**, 109–139 (2008)
2. Cosnier, S., Mailley, P.: Recent advances in DNA sensors. Analyst **133**, 984–991 (2008)
3. Vercoutere, W., Akeson, M.: Biosensors for DNA sequence detection. Curr. Opin. Chem. Biol. **6**, 816–822 (2002)
4. Teles, F.R.R., Fonseca, L.R.: Trends in DNA biosensors. Talanta **77**, 606–623 (2008)
5. Song, S.P., Qin, Y., He, Y., Huang, Q., Fan, C.H., Chen, H.Y.: Functional nanoprobes for ultrasensitive detection of biomolecules. Chem. Soc. Rev. **39**, 4234–4243 (2010)
6. Li, D., Song, S.P., Fan, C.H.: Target-responsive structural switching for nucleic acid-based sensors. Acc. Chem. Res. **43**, 631–641 (2010)
7. Rosi, N.L., Mirkin, C.A.: Nanostructures in biodiagnostics. Chem. Rev. **105**, 1547–1562 (2005)
8. Elghanian, R., Storhoff, J.J., Mucic, R.C., Letsinger, R.L., Mirkin, C.A.: Selective colorimetric detection of polynucleotides based on the distance-dependent optical properties of gold nanoparticles. Science **277**, 1078–1081 (1997)
9. Mirkin, C.A., Letsinger, R.L., Mucic, R.C., Storhoff, J.J.: A DNA-based method for rationally assembling nanoparticles into macroscopic materials. Nature **382**, 607–609 (1996)
10. Wilson, R.: The use of gold nanoparticles in diagnostics and detection. Chem. Soc. Rev. **37**, 2028–2045 (2008)
11. Edwards, P.P., Thomas, J.M.: Gold in a metallic divided state – from Faraday to present-day nanoscience. Angew. Chem. Int. Ed. **46**, 5480–5486 (2007)
12. Reynolds, R.A., Mirkin, C.A., Letsinger, R.L.: Homogeneous, nanoparticle-based quantitative colorimetric detection of oligonucleotides. J. Am. Chem. Soc. **122**, 3795–3796 (2000)
13. Jin, R.C., Wu, G.S., Li, Z., Mirkin, C.A., Schatz, G.C.: What controls the melting properties of DNA-linked gold nanoparticle assemblies? J. Am. Chem. Soc. **125**, 1643–1654 (2003)
14. Zhao, W., Brook, M.A., Li, Y.F.: Design of gold nanoparticle-based colorimetric biosensing assays. ChemBioChem **9**, 2363–2371 (2008)

15. Dai, Z., Zhang, J.M., Dong, Q.X., Guo, N., Xu, S.C., Sun, B., Bu, Y.H.: Adaption of Au nanoparticles and CdTe quantum dots in DNA detection. Chin. J. Chem. Eng. **15**, 791–794 (2007)
16. Taton, T.A., Mirkin, C.A., Letsinger, R.L.: Scanometric DNA array detection with nanoparticle probes. Science **289**, 1757–1760 (2000)
17. Li, H.X., Rothberg, L.: Colorimetric detection of DNA sequences based on electrostatic interactions with unmodified gold nanoparticles. Proc. Natl. Acad. Sci. USA **101**, 14036–14039 (2004)
18. Li, H.X., Rothberg, L.: Detection of specific sequences in RNA using differential adsorption of single-stranded oligonucleotides on gold nanoparticles. Anal. Chem. **77**, 6229–6233 (2005)
19. Li, H.X., Rothberg, L.J.: Label-free colorimetric detection of specific sequences in genomic DNA amplified by the polymerase chain reaction. J. Am. Chem. Soc. **126**, 10958–10961 (2004)
20. Wang, L.H., Liu, X.F., Hu, X.F., Song, S.P., Fan, C.H.: Unmodified gold nanoparticles as a colorimetric probe for potassium DNA aptamers. Chem. Commun. 3780–3782 (2006)
21. Wang, J., Wang, L.H., Liu, X.F., Liang, Z.Q., Song, S.P., Li, W.X., Li, G.X., Fan, C.H.: A gold nanoparticle-based aptamer target binding readout for ATP assay. Adv. Mater. **19**, 3943–3946 (2007)
22. Zhang, J., Wang, L.H., Pan, D., Song, S.P., Boey, F.Y.C., Zhang, H., Fan, C.H.: Visual cocaine detection with gold nanoparticles and rationally engineered aptamer structures. Small **4**, 1196–1200 (2008)
23. Tyagi, S., Kramer, F.R.: Molecular beacons: probes that fluoresce upon hybridization. Nat. Biotechnol. **14**, 303–308 (1996)
24. Wang, K.M., Tang, Z.W., Yang, C.Y.J., Kim, Y.M., Fang, X.H., Li, W., Wu, Y.R., Medley, C.D., Cao, Z.H., Li, J., Colon, P., Lin, H., Tan, W.H.: Molecular engineering of DNA: molecular beacons. Angew. Chem. Int. Ed. **48**, 856–870 (2009)
25. Tan, W.H., Wang, K.M., Drake, T.J.: Molecular beacons. Curr. Opin. Chem. Biol. **8**, 547–553 (2004)
26. Marras, S.A.E., Tyagi, S., Kramer, F.R.: Real-time assays with molecular beacons and other fluorescent nucleic acid hybridization probes. Clin. Chim. Acta **363**, 48–60 (2006)
27. Whitcombe, D., Theaker, J., Guy, S.P., Brown, T., Little, S.: Detection of PCR products using self-probing amplicons and fluorescence. Nat. Biotechnol. **17**, 804–807 (1999)
28. Wittwer, C.T., Herrmann, M.G., Gundry, C.N., Elenitoba-Johnson, K.S.J.: Real-time multiplex PCR assays. Methods **25**, 430–442 (2001)
29. Wabuyele, M.B., Farquar, H., Stryjewski, W., Hammer, R.P., Soper, S.A., Cheng, Y.W., Barany, F.: Approaching real-time molecular diagnostics: single-pair fluorescence resonance energy transfer (spFRET) detection for the analysis of low abundant point mutations in K-ras oncogenes. J. Am. Chem. Soc. **125**, 6937–6945 (2003)
30. Wong, M.L., Medrano, J.F.: Real-time PCR for mRNA quantitation. Biotechniques **39**, 75–85 (2005)
31. Santangelo, P.J., Nix, B., Tsourkas, A., Bao, G.: Dual FRET molecular beacons for mRNA detection in living cells. Nucleic Acids Res. **32**(9) (2004)
32. Bratu, D.P., Cha, B.J., Mhlanga, M.M., Kramer, F.R., Tyagi, S.: Visualizing the distribution and transport of mRNAs in living cells. Proc. Natl. Acad. Sci. USA **100**, 13308–13313 (2003)
33. Kiesling, T., Cox, K., Davidson, E.A., Dretchen, K., Grater, G., Hibbard, S., Lasken, R.S., Leshin, J., Skowronski, E., Danielsen, M.: Sequence specific detection of DNA using nicking endonuclease signal amplification (NESA). Nucleic Acids Res. **35**, 9 (2007)
34. Li, J.W.J., Chu, Y.Z., Lee, B.Y.H., Xie, X.L.S.: Enzymatic signal amplification of molecular beacons for sensitive DNA detection. Nucleic Acids Res. **36**, 17 (2008)
35. Xu, W., Xue, X.J., Li, T.H., Zeng, H.Q., Liu, X.G.: Ultrasensitive and selective colorimetric DNA detection by nicking endonuclease assisted nanoparticle amplification. Angew. Chem. Int. Ed. **48**, 6849–6852 (2009)
36. Zhou, B.J., Ma, Y.J., Wu, H.P., Zhou, G.H.: Ultrasensitive DNA detection by cascade enzymatic signal amplification based on Afu Flap endonuclease coupled with nicking endonuclease. Angew. Chem. Int. Ed. **50**, 7395–7398 (2011)

37. Zuo, X.L., Xia, F., Xiao, Y., Plaxco, K.W.: Sensitive and selective amplified fluorescence DNA detection based on Exonuclease III-aided target recycling. J. Am. Chem. Soc. **132**, 1816–1818 (2010)
38. Zhao, X.J., Bagwe, R.P., Tan, W.H.: Development of organic-dye-doped silica nanoparticles in a reverse microemulsion. Adv. Mater. **16**, 173–176 (2004)
39. Yan, J.L., Estevez, M.C., Smith, J.E., Wang, K.M., He, X.X., Wang, L., Tan, W.H.: Dye-doped nanoparticles for bioanalysis. Nano Today **2**, 44–50 (2007)
40. Zhao, X.J., Tapec-Dytioco, R., Tan, W.H.: Ultrasensitive DNA detection using highly fluorescent bioconjugated nanoparticles. J. Am. Chem. Soc. **125**, 11474–11475 (2003)
41. Zhou, X.C., Zhou, J.Z.: Improving the signal sensitivity and photostability of DNA hybridizations on microarrays by using dye-doped core-shell silica nanoparticles. Anal. Chem. **76**, 5302–5312 (2004)
42. Yin, Y., Alivisatos, A.P.: Colloidal nanocrystal synthesis and the organic-inorganic interface. Nature **437**, 664–670 (2005)
43. Peng, Z.A., Peng, X.G.: Formation of high-quality CdTe, CdSe, and CdS nanocrystals using CdO as precursor. J. Am. Chem. Soc. **123**, 183–184 (2001)
44. Algar, W.R., Massey, M., Krull, U.J.: The application of quantum dots, gold nanoparticles and molecular switches to optical nucleic-acid diagnostics. TrAC Trends Anal. Chem. **28**, 292–306 (2009)
45. Sutherland, A.J.: Quantum dots as luminescent probes in biological systems. Curr. Opin. Solid State Mater. Sci. **6**, 365–370 (2002)
46. Han, M.Y., Gao, X.H., Su, J.Z., Nie, S.: Quantum-dot-tagged microbeads for multiplexed optical coding of biomolecules. Nat. Biotechnol. **19**, 631–635 (2001)
47. Clapp, A.R., Medintz, I.L., Mattoussi, H.: Forster resonance energy transfer investigations using quantum-dot fluorophores. ChemPhysChem **7**, 47–57 (2006)
48. Clapp, A.R., Medintz, I.L., Uyeda, H.T., Fisher, B.R., Goldman, E.R., Bawendi, M.G., Mattoussi, H.: Quantum dot-based multiplexed fluorescence resonance energy transfer. J. Am. Chem. Soc. **127**, 18212–18221 (2005)
49. Kim, J.H., Morikis, D., Ozkan, M.: Adaptation of inorganic quantum dots for stable molecular beacons. Sens. Actuator B Chem. **102**, 315–319 (2004)
50. Algar, W.R., Krull, U.J.: Towards multi-colour strategies for the detection of oligonucleotide hybridization using quantum dots as energy donors in fluorescence resonance energy transfer (FRET). Anal. Chim. Acta **581**, 193–201 (2007)
51. Zhang, C.Y., Yeh, H.C., Kuroki, M.T., Wang, T.H.: Single-quantum-dot-based DNA nanosensor. Nat. Mater. **4**, 826–831 (2005)
52. Peng, H., Zhang, L.J., Kjallman, T.H.M., Soeller, C., Travas-Sejdic, J.: DNA hybridization detection with blue luminescent quantum dots and dye-labeled single-stranded DNA. J. Am. Chem. Soc. **129**, 3048–3049 (2007)
53. Su, Y.Y., Hu, M., Fan, C.H., He, Y., Li, Q.N., Li, W.X., Wang, L.H., Shen, P.P., Huang, Q.: The cytotoxicity of CdTe quantum dots and the relative contributions from released cadmium ions and nanoparticle properties. Biomaterials **31**, 4829–4834 (2010)
54. Jurbergs, D., Rogojina, E., Mangolini, L., Kortshagen, U.: Silicon nanocrystals with ensemble quantum yields exceeding 60 %. Appl. Phys. Lett. **88**, 23316 (2006)
55. He, Y., Kang, Z.H., Li, Q.S., Tsang, C.H.A., Fan, C.H., Lee, S.T.: Ultrastable, highly fluorescent, and water-dispersed silicon-based nanospheres as cellular probes. Angew. Chem. Int. Ed. **48**, 128–132 (2009)
56. He, Y., Su, Y.Y., Yang, X.B., Kang, Z.H., Xu, T.T., Zhang, R.Q., Fan, C.H., Lee, S.T.: Photo and pH stable, highly-luminescent silicon nanospheres and their bioconjugates for immunofluorescent cell imaging. J. Am. Chem. Soc. **131**, 4434–4438 (2009)
57. Zijlmans, H., Bonnet, J., Burton, J., Kardos, K., Vail, T., Niedbala, R.S., Tanke, H.J.: Detection of cell and tissue surface antigens using up-converting phosphors: a new reporter technology. Anal. Biochem. **267**, 30–36 (1999)

58. Kamimura, M., Miyamoto, D., Saito, Y., Soga, K., Nagasaki, Y.: Design of poly(ethylene glycol)/streptavidin coimmobilized upconversion nanophosphors and their application to fluorescence biolabeling. Langmuir **24**, 8864–8870 (2008)
59. Emoto, K., Nagasaki, Y., Kataoka, K.: Coating of surfaces with stabilized reactive micelles from poly(ethylene glycol)-poly(DL-lactic acid) block copolymer. Langmuir **15**, 5212–5218 (1999)
60. van de Rijke, F., Zijlmans, H., Li, S., Vail, T., Raap, A.K., Niedbala, R.S., Tanke, H.J.: Up-converting phosphor reporters for nucleic acid microarrays. Nat. Biotechnol. **19**, 273–276 (2001)
61. Chen, Z.G., Chen, H.L., Hu, H., Yu, M.X., Li, F.Y., Zhang, Q., Zhou, Z.G., Yi, T., Huang, C.H.: Versatile synthesis strategy for carboxylic acid-functionalized upconverting nanophosphors as biological labels. J. Am. Chem. Soc. **130**, 3023–3029 (2008)
62. Dulkeith, E., Morteani, A.C., Niedereichholz, T., Klar, T.A., Feldmann, J., Levi, S.A., van Veggel, F., Reinhoudt, D.N., Moller, M., Gittins, D.I.: Fluorescence quenching of dye molecules near gold nanoparticles: radiative and nonradiative effects. Phys. Rev. Lett. **89**, 4 (2002)
63. Das, P.C., Puri, A.: Energy flow and fluorescence near a small metal particle. Phys. Rev. B **65**, 8 (2002)
64. Fan, C.H., Wang, S., Hong, J.W., Bazan, G.C., Plaxco, K.W., Heeger, A.J.: Beyond superquenching: hyper-efficient energy transfer from conjugated polymers to gold nanoparticles. Proc. Natl. Acad. Sci. USA **100**, 6297–6301 (2003)
65. Kamat, P.V., Barazzouk, S., Hotchandani, S.: Electrochemical modulation of fluorophore emission on a nanostructured gold film. Angew. Chem. Int. Ed. **41**, 2764–2767 (2002)
66. Dubertret, B., Calame, M., Libchaber, A.J.: Single-mismatch detection using gold-quenched fluorescent oligonucleotides. Nat. Biotechnol. **19**, 365–370 (2001)
67. Maxwell, D.J., Taylor, J.R., Nie, S.M.: Self-assembled nanoparticle probes for recognition and detection of biomolecules. J. Am. Chem. Soc. **124**, 9606–9612 (2002)
68. Song, S.P., Liang, Z.Q., Zhang, J., Wang, L.H., Li, G.X., Fan, C.H.: Gold-nanoparticle-based multicolor nanobeacons for sequence-specific DNA analysis. Angew. Chem. Int. Ed. **48**, 8670–8674 (2009)
69. Pons, T., Medintz, I.L., Sapsford, K.E., Higashiya, S., Grimes, A.F., English, D.S., Mattoussi, H.: On the quenching of semiconductor quantum dot photoluminescence by proximal gold nanoparticles. Nano Lett. **7**, 3157–3164 (2007)
70. Zheng, M., Jagota, A., Semke, E.D., Diner, B.A., McLean, R.S., Lustig, S.R., Richardson, R.E., Tassi, N.G.: DNA-assisted dispersion and separation of carbon nanotubes. Nat. Mater. **2**, 338–342 (2003)
71. Zheng, M., Jagota, A., Strano, M.S., Santos, A.P., Barone, P., Chou, S.G., Diner, B.A., Dresselhaus, M.S., McLean, R.S., Onoa, G.B., Samsonidze, G.G., Semke, E.D., Usrey, M., Walls, D.J.: Structure-based carbon nanotube sorting by sequence-dependent DNA assembly. Science **302**, 1545–1548 (2003)
72. Liang, F., Chen, B.: A review on biomedical applications of single-walled carbon nanotubes. Curr. Med. Chem. **17**, 10–24 (2010)
73. Zhu, Z., Yang, R.H., You, M.X., Zhang, X.L., Wu, Y.R., Tan, W.H.: Single-walled carbon nanotube as an effective quencher. Anal. Bioanal. Chem. **396**, 73–83 (2010)
74. Yang, R.H., Tang, Z.W., Yan, J.L., Kang, H.Z., Kim, Y.M., Zhu, Z., Tan, W.H.: Noncovalent assembly of carbon nanotubes and single-stranded DNA: an effective sensing platform for probing biomolecular interactions. Anal. Chem. **80**, 7408–7413 (2008)
75. Yang, R.H., Jin, J.Y., Chen, Y., Shao, N., Kang, H.Z., Xiao, Z., Tang, Z.W., Wu, Y.R., Zhu, Z., Tan, W.H.: Carbon nanotube-quenched fluorescent oligonucleotides: probes that fluoresce upon hybridization. J. Am. Chem. Soc. **130**, 8351–8358 (2008)
76. Liu, Y., Wang, Y.X., Jin, J.Y., Wang, H., Yang, R.H., Tan, W.H.: Fluorescent assay of DNA hybridization with label-free molecular switch: reducing background-signal and improving specificity by using carbon nanotubes. Chem. Commun. 665–667 (2009)

77. Rao, C.N.R., Sood, A.K., Subrahmanyam, K.S., Govindaraj, A.: Graphene: the new two-dimensional nanomaterial. Angew. Chem. Int. Ed. **48**, 7752–7777 (2009)
78. Dreyer, D.R., Park, S., Bielawski, C.W., Ruoff, R.S.: The chemistry of graphene oxide. Chem. Soc. Rev. **39**, 228–240 (2010)
79. Swathi, R.S., Sebastian, K.L.: Resonance energy transfer from a dye molecule to graphene. J. Chem. Phys. **129**, 9 (2008)
80. He, S.J., Song, B., Li, D., Zhu, C.F., Qi, W.P., Wen, Y.Q., Wang, L.H., Song, S.P., Fang, H.P., Fan, C.H.: A graphene nanoprobe for rapid, sensitive, and multicolor fluorescent DNA analysis. Adv. Funct. Mater. **20**, 453–459 (2010)
81. Lu, C.H., Yang, H.H., Zhu, C.L., Chen, X., Chen, G.N.: A graphene platform for sensing biomolecules. Angew. Chem. Int. Ed. **48**, 4785–4787 (2009)
82. Wang, Y., Li, Z.H., Hu, D.H., Lin, C.T., Li, J.H., Lin, Y.H.: Aptamer/graphene oxide nanocomplex for in situ molecular probing in living cells. J. Am. Chem. Soc. **132**, 9274–9276 (2010)
83. Feng, L.Z., Zhang, S.A., Liu, Z.: Graphene based gene transfection. Nanoscale **3**, 1252–1257 (2011)
84. Peng, C., Hu, W.B., Zhou, Y.T., Fan, C.H., Huang, Q.: Intracellular imaging with a graphene-based fluorescent probe. Small **6**, 1686–1692 (2010)
85. Gerardi, R.D., Barnett, N.W., Lewis, S.W.: Analytical applications of tris(2,2′-bipyridyl)ruthenium(III) as a chemiluminescent reagent. Anal. Chim. Acta **378**, 1–41 (1999)
86. Dodeigne, C., Thunus, L., Lejeune, R.: Chemiluminescence as a diagnostic tool. A review. Talanta **51**, 415–439 (2000)
87. Marquette, C.A., Blum, L.J.: Electro-chemiluminescent biosensing. Anal. Bioanal. Chem. **390**, 155–168 (2008)
88. Kricka, L.J.: Clinical applications of chemiluminescence. Anal. Chim. Acta **500**, 279–286 (2003)
89. Aslan, K., Geddes, C.D.: Metal-enhanced chemiluminescence: advanced chemiluminescence concepts for the 21st century. Chem. Soc. Rev. **38**, 2556–2564 (2009)
90. Lin, J.M., Shan, X.Q., Hanaoka, S., Yamada, M.: Luminol chemiluminescence in unbuffered solutions with a cobalt(II)-ethanolamine complex immobilized on resin as catalyst and its application to analysis. Anal. Chem. **73**, 5043–5051 (2001)
91. Li, Z.P., Li, K.A., Tong, S.Y.: Study of the catalytic effect of copper(II)-protein complexes on luminol-H2O2 chemiluminescence reaction and its analytical application. Anal. Lett. **32**, 901–913 (1999)
92. Zhang, S.S., Zhong, H., Ding, C.F.: Ultrasensitive flow injection chemiluminescence detection of DNA hybridization using signal DNA probe modified with Au and CuS nanoparticles. Anal. Chem. **80**, 7206–7212 (2008)
93. Niazov, T., Pavlov, V., Xiao, Y., Gill, R., Willner, I.: DNAzyme-functionalized Au nanoparticles for the amplified detection of DNA or telomerase activity. Nano Lett. **4**, 1683–1687 (2004)
94. Wang, Z.P., Hu, J.Q., Jin, Y., Yao, X., Li, J.H.: In situ amplified chemiluminescent detection of DNA and immunoassay of IgG using special-shaped gold nanoparticles as label. Clin. Chem. **52**, 1958–1961 (2006)
95. Qi, Y.Y., Li, B.X., Zhang, Z.J.: Label-free and homogeneous DNA hybridization detection using gold nanoparticles-based chemiluiminescence system. Biosens. Bioelectron. **24**, 3581–3586 (2009)
96. Nelson, N.C., BenCheikh, A., Matsuda, E., Becker, M.M.: Simultaneous detection of multiple nucleic acid targets in a homogeneous format. Biochemistry **35**, 8429–8438 (1996)
97. Nelson, N.C., Kacian, D.L.: Chemiluminescent DNA probes-A comparison of the acridinium and dioxetane detection systems and their use in clinical diagnostic assays. Clin. Chim. Acta **194**, 73–90 (1990)
98. Nelson, N.C., Hammond, P.W., Matsuda, E., Goud, A.A., Becker, M.M.: Detection of all single-base mismatches in solution by chemiluminescence. Nucleic Acids Res. **24**, 4998–5003 (1996)

99. Yin, X.B., Dong, S.J., Wang, E.K.: Analytical applications of the electrochemiluminescence of tris (2.2′-bipyridyl) ruthenium and its derivatives. TrAC Trends Anal. Chem. **23**, 432–441 (2004)
100. Hu, L.Z., Xu, G.B.: Applications and trends in electrochemiluminescence. Chem. Soc. Rev. **39**, 3275–3304 (2010)
101. Tokel, N.E., Bard, A.J.: Electrogenerated chemiluminescence. 9. electrochemistry and emission from systems containing Tris(2,2′-bipyridine)Ruthenium(II) dichloride. J. Am. Chem. Soc **94**, 2862–2863 (1972)
102. Zu, Y.B., Bard, A.J.: Electrogenerated chemiluminescence. 66. The role of direct coreactant oxidation in the ruthenium tris(2,2′)bipyridyl/tripropylamine system and the effect of halide ions on the emission intensity. Anal. Chem. **72**, 3223–3232 (2000)
103. Kanoufi, F., Zu, Y.B., Bard, A.J.: Homogeneous oxidation of trialkylamines by metal complexes and its impact on electrogenerated chemiluminescence in the trialkylamine/$Ru(bpy)_{(3)}^{(2+)}$ system. J. Phys. Chem. B **105**, 210–216 (2001)
104. Miao, W.J.: Electrogenerated chemiluminescence and its biorelated applications. Chem. Rev. **108**, 2506–2553 (2008)
105. Xu, X.H., Bard, A.J.: Immobilization and hybridization of DNA and Aluminum (III) alkanebisphosphonate thin-film with electrogenerated chemiluminescent detection. J. Am. Chem. Soc. **117**, 2627–2631 (1995)
106. Miao, W.J., Bard, A.J.: Electrogenerated chemiluminescence. 77. DNA hybridization detection at high amplification with [Ru(bpy)(3)](2+)-containing microspheres. Anal. Chem. **76**, 5379–5386 (2004)
107. Miao, W.J., Bard, A.J.: Electrogenerated chemluminescence. 72. Determination of immobilized DNA and C-reactive protein on Au(111) electrodes using Tris(2,2′-bipyridyl)ruthenium(II) labels. Anal. Chem. **75**, 5825–5834 (2003)
108. Lo, W.Y., Baeumner, A.J.: Evaluation of internal standards in a competitive nucleic acid sequence-based amplification assay. Anal. Chem. **79**, 1386–1392 (2007)
109. Lo, W.Y., Baeumner, A.J.: RNA internal standard synthesis by nucleic acid sequence-based amplification for competitive quantitative amplification reactions. Anal. Chem. **79**, 1548–1554 (2007)
110. Zhang, J., Qi, H.L., Li, Y., Yang, J., Gao, Q., Zhang, C.X.: Electrogenerated chemiluminescence DNA biosensor based on hairpin DNA probe labeled with ruthenium complex. Anal. Chem. **80**, 2888–2894 (2008)
111. Sun, X.P., Du, Y., Dong, S.J., Wang, E.K.: Method for effective immobilization of $Ru(bpy)_3^{2+}$ on an electrode surface for solid-state electrochemiluminescene detection. Anal. Chem. **77**, 8166–8169 (2005)
112. Wang, H., Zhang, C.X., Li, Y., Qi, H.L.: Electrogenerated chemiluminescence detection for deoxyribonucleic acid hybridization based on gold nanoparticles carrying multiple probes. Anal. Chim. Acta **575**, 205–211 (2006)
113. Zhang, J., Song, S.P., Zhang, L.Y., Wang, L.H., Wu, H.P., Pan, D., Fan, C.H.: Sequence-specific detection of femtomolar DNA via a chronocoulometric DNA sensor (CDS): effects of nanoparticle-mediated amplification and nanoscale control of DNA assembly at electrodes. J. Am. Chem. Soc. **128**, 8575–8580 (2006)
114. Lee, J.G., Yun, K., Lim, G.S., Lee, S.E., Kim, S., Park, J.K.: DNA biosensor based on the electrochemiluminescence of $Ru(bpy)_{(3)}^{(2+)}$ with DNA-binding intercalators. Bioelectrochemistry **70**, 228–234 (2007)
115. Jiang, H., Ju, H.X.: Enzyme-quantum dots architecture for highly sensitive electrochemiluminescence biosensing of oxidase substrates. Chem. Commun. 404–406 (2007)
116. Jiang, H., Ju, H.X.: Electrochemiluminescence sensors for scavengers of hydroxyl radical based on its annihilation in CdSe quantum dots film/peroxide system. Anal. Chem. **79**, 6690–6696 (2007)
117. Liu, X., Jiang, H., Lei, J.P., Ju, H.X.: Anodic electrochemiluminescence of CdTe quantum dots and its energy transfer for detection of catechol derivatives. Anal. Chem. **79**, 8055–8060 (2007)

118. Hu, X.F., Wang, R.Y., Ding, Y., Zhang, X.L., Jin, W.R.: Electrochemiluminescence of CdTe quantum dots as labels at nanoporous gold leaf electrodes for ultrasensitive DNA analysis. Talanta **80**, 1737–1743 (2010)
119. Fivash, M., Towler, E.M., Fisher, R.J.: BIAcore for macromolecular interaction. Curr. Opin. Biotechnol. **9**, 97–101 (1998)
120. Malmborg, A.C., Borrebaeck, C.A.K.: BIAcore as a tool in antibody engineering. J. Immunol. Methods **183**, 7–13 (1995)
121. Campbell, C.T., Kim, G.: SPR microscopy and its applications to high-throughput analyses of biomolecular binding events and their kinetics. Biomaterials **28**, 2380–2392 (2007)
122. Homola, J.: Surface plasmon resonance sensors for detection of chemical and biological species. Chem. Rev. **108**, 462–493 (2008)
123. Homola, J., Yee, S.S., Gauglitz, G.: Surface plasmon resonance sensors: review. Sens. Actuator B Chem. **54**, 3–15 (1999)
124. Persson, B., Stenhag, K., Nilsson, P., Larsson, A., Uhlen, M., Nygren, P.A.: Analysis of oligonucleotide probe affinities using surface plasmon resonance: a means for mutational scanning. Anal. Biochem. **246**, 34–44 (1997)
125. Nilsson, P., Persson, B., Uhlen, M., Nygren, P.A.: Real-time monitoring of DNA manipulations using biosensor technology. Anal. Biochem. **224**, 400–408 (1995)
126. He, L., Musick, M.D., Nicewarner, S.R., Salinas, F.G., Benkovic, S.J., Natan, M.J., Keating, C.D.: Colloidal Au-enhanced surface plasmon resonance for ultrasensitive detection of DNA hybridization. J. Am. Chem. Soc. **122**, 9071–9077 (2000)
127. Rothenhausler, B., Knoll, W.: Surface-plasmon microscopy. Nature **332**, 615–617 (1988)
128. Shumaker-Parry, J.S., Zareie, M.H., Aebersold, R., Campbell, C.T.: Microspotting streptavidin and double-stranded DNA Arrays on gold for high-throughput studies of protein-DNA interactions by surface plasmon resonance microscopy. Anal. Chem. **76**, 918–929 (2004)
129. Brockman, J.M., Nelson, B.P., Corn, R.M.: Surface plasmon resonance imaging measurements of ultrathin organic films. Annu. Rev. Phys. Chem. **51**, 41–63 (2000)
130. Thiel, A.J., Frutos, A.G., Jordan, C.E., Corn, R.M., Smith, L.M.: In situ surface plasmon resonance imaging detection of DNA hybridization to oligonucleotide arrays on gold surfaces. Anal. Chem. **69**, 4948–4956 (1997)
131. Nelson, B.P., Grimsrud, T.E., Liles, M.R., Goodman, R.M., Corn, R.M.: Surface plasmon resonance imaging measurements of DNA and RNA hybridization adsorption onto DNA microarrays. Anal. Chem. **73**, 1–7 (2001)
132. Jordan, C.E., Frutos, A.G., Thiel, A.J., Corn, R.M.: Surface plasmon resonance imaging measurements of DNA hybridization adsorption and streptavidin/DNA multilayer formation at chemically modified gold surfaces. Anal. Chem. **69**, 4939–4947 (1997)
133. Lee, H.J., Goodrich, T.T., Corn, R.M.: SPR imaging measurements of 1-D and 2-D DNA microarrays created from microfluidic channels on gold thin films. Anal. Chem. **73**, 5525–5531 (2001)
134. Lee, H.J., Li, Y., Wark, A.W., Corn, R.M.: Enzymatically amplified surface plasmon resonance imaging detection of DNA by exonuclease III digestion of DNA microarrays. Anal. Chem. **77**, 5096–5100 (2005)
135. Nie, S.M., Emery, S.R.: Probing single molecules and single nanoparticles by surface-enhanced Raman scattering. Science **275**, 1102–1106 (1997)
136. Vodinh, T., Houck, K., Stokes, D.L.: PROBES surface-enhanced Raman gene probes. Anal. Chem. **66**, 3379–3383 (1994)
137. Campion, A., Kambhampati, P.: Surface-enhanced Raman scattering. Chem. Soc. Rev. **27**, 241–250 (1998)
138. Graham, D.: The next generation of advanced spectroscopy: surface enhanced Raman scattering from metal nanoparticles. Angew. Chem. Int. Ed. **49**, 9325–9327 (2010)
139. Graham, D., Faulds, K.: Quantitative SERRS for DNA sequence analysis. Chem. Soc. Rev. **37**, 1042–1051 (2008)
140. Cao, Y.W.C., Jin, R.C., Mirkin, C.A.: Nanoparticles with Raman spectroscopic fingerprints for DNA and RNA detection. Science **297**, 1536–1540 (2002)

141. Braun, G., Lee, S.J., Dante, M., Nguyen, T.Q., Moskovits, M., Reich, N.: Surface-enhanced Raman spectroscopy for DNA detection by nanoparticle assembly onto smooth metal films. J. Am. Chem. Soc. **129**, 6378–6379 (2007)
142. Kang, T., Yoo, S.M., Yoon, I., Lee, S.Y., Kim, B.: Patterned multiplex pathogen DNA detection by Au particle-on-wire SERS sensor. Nano Lett. **10**, 1189–1193 (2010)
143. He, Y., Su, S., Xu, T.T., Zhong, Y.L., Antonio Zapien, J., Li, J., Fan, C.H., Lee, S.-T.: Silicon nanowires-based highly-efficient SERS-active platform for ultrasensitive DNA detection. Nano Today **6**, 122–130 (2011)
144. Thompson, D.G., Enright, A., Faulds, K., Smith, W.E., Graham, D.: Ultrasensitive DNA detection using oligonucleotide-silver nanoparticle conjugates. Anal. Chem. **80**, 2805–2810 (2008)
145. MacAskill, A., Crawford, D., Graham, D., Faulds, K.: DNA sequence detection using surface-enhanced resonance Raman spectroscopy in a homogeneous multiplexed assay. Anal. Chem. **81**, 8134–8140 (2009)
146. Graham, D., Stevenson, R., Thompson, D.G., Barrett, L., Dalton, C., Faulds, K.: Combining functionalized nanoparticles and SERS for the detection of DNA relating to disease. Faraday Discuss. **149**, 291–299 (2010)
147. Graham, D., Thompson, D.G., Smith, W.E., Faulds, K.: Control of enhanced Raman scattering using a DNA-based assembly process of dye-coded nanoparticles. Nat. Nanotechnol. **3**, 548–551 (2008)
148. Wabuyele, M.B., Vo-Dinh, T.: Detection of human immunodeficiency virus type 1 DNA sequence using plasmonics nanoprobes. Anal. Chem. **77**, 7810–7815 (2005)
149. Harpster, M.H., Zhang, H., Sankara-Warrier, A.K., Ray, B.H., Ward, T.R., Kollmar, J.P., Carron, K.T., Mecham, J.O., Corcoran, R.C., Wilson, W.C., Johnson, P.A.: SERS detection of indirect viral DNA capture using colloidal gold and methylene blue as a Raman label. Biosens. Bioelectron. **25**, 674–681 (2009)
150. Zhang, Z., Wang, Y., Fan, C.H., Li, C., Li, Y., Qian, L.L., Fu, Y.M., Shi, Y.Y., Hu, J., He, L.: Asymmetric DNA origami for spatially addressable and index-free solution-phase DNA chips. Adv. Mater. **22**, 2672–2675 (2010)
151. Ke, Y.G., Lindsay, S., Chang, Y., Liu, Y., Yan, H.: Self-assembled water-soluble nucleic acid probe tiles for label-free RNA hybridization assays. Science **319**, 180–183 (2008)
152. Husale, S., Persson, H.H.J., Sahin, O.: DNA nanomechanics allows direct digital detection of complementary DNA and microRNA targets. Nature **462**, 1075–1078 (2009)